Math. Proc. Camb. Phil. Soc. (1976), **79**, 343
With 7 text-figures
MPCPS 79-29
Printed in Great Britain

A higher catastrophe machine

BY A. E. R. WOODCOCK†
IBM Thomas J. Watson Research Centre, Yorktown Heights, New York 10598 *U.S.A.*

AND TIM POSTON
University of Rochester, Department of Mathematics, Rochester, New York 14627, *U.S.A.*

(*Received* 13 *December* 1974)

Abstract. An elaborated version of Zeeman's Catastrophe Machine (1), which physically illustrates the butterfly catastrophe, is described and analyzed.

In (1) the cusp catastrophe was illustrated by an analysis of Zeeman's catastrophe machine (2). A number of such illustrations of this two-dimensional catastrophe, widely different in the forms of potential energy made use of, have been constructed. However, machines to illustrate the higher catastrophes (swallowtail, butterfly and three umbilics – see, for example, (3)) have been lacking. We describe here a development of the Zeeman machine due to Bill Barit (4), the description of whose behaviour involves a four-dimensional catastrophe.

Recall that the original machine consists of a wheel of radius, r, free to turn about the origin O, with two elastic strings of unstretched length P attached to a point B on its edge. The lower has its second end at a fixed point $A = (O, -a)$, the upper at a variable point $X = (x, y)$ (Fig. 1). The Butterfly Machine (Fig. 2) has a wheel mounted similarly but controlled differently. In place of BX it has a double elastic string of unstretched length J (thus doubling the force produced by a single string). In place of BA, it has a pair of elastic strings BA_+, BA_- of unstretched lengths P, Q attached to points A_+, A_- both at distance a from O, angles $+\phi$, $-\phi$ respectively from the downward y-axis. We specify $P+Q = 4R$ and fix $J = 2R$ to reduce dimension; it is clear that when $P = Q = J$ and $\phi = 0$, the system is equivalent to the Zeeman machine. Figure 4*a* was drawn with $J = R$ and $\phi = 0$. We consider only the region C of those values (x, y, P, ϕ) for which all the strings are under tension for all θ.

In place of the two control variables x, y of (1), we now have four: x, y, P or Q, ϕ. With all of these fixed, there are one or more values of θ for which the wheel is in equilibrium, (stable or unstable), and we are concerned with the singularities of the map

$$S = \{(x, y, P, \phi, \theta) | \text{ wheel in equilibrium at } \theta\} \to C$$
$$(x, y, p, \phi, \theta) \overset{\chi}{\rightsquigarrow} (x, y, p, \phi).$$

† Present address: Williams College, Department of Biology, Williamstown, Massachusetts 01267, U.S.A.

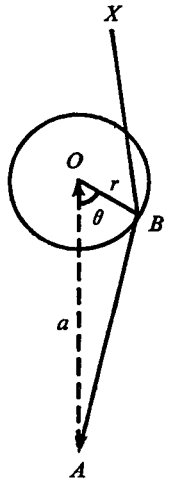

Fig. 1

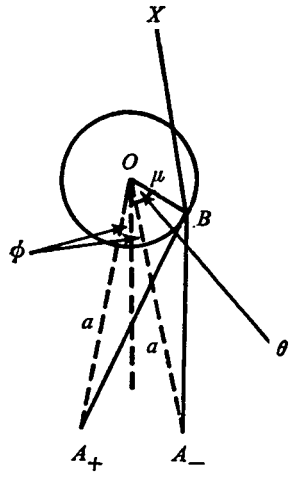

Fig. 2

Fig. 1. Diagram of the Mk I Zeeman Catastrophe Machine with single lower elastic. Disc, radius r, centre O, distance a from lower elastic connexion attached at B, for further details, see text.

Fig. 2. Configuration of the Higher Catastrophe Machine. Two elastic strings attached at A_+ and A_- respectively and at B on the disc centre O radius μ. Angle A_+OA_- is 2ϕ; for further details, see text.

We assume the function V, assigning to each (x, y, P, ϕ, θ) the corresponding elastic energy of the system, to be generic. The local diffeotype of the singularity we are concerned with must then be that of one of the first four cuspoid catastrophes, since the behaviour space of the system (the S^1 values of θ) is one-dimensional and C is four-dimensional. The theorem is proved for this restricted case in (5); the most accessible self-contained proof of the general, higher dimensional behaviour case which includes the umbilic catastrophes is (6). The computer-generated pictures that follow make it clear that the catastrophe concerned is the butterfly. (It would be of interest to have the local equivalence involved displayed in detail, as has been done for the lower cusp of the Zeeman machine (7)).

Now if we fix P, ϕ and θ, the values that (x, y) may take are governed by the same considerations as in (1). Their locus must thus be a conchoid of Nichomedes or, in the variation analogous to the Mk II machine, straight lines. The somewhat more complicated law for the downward force on the wheel gives a more complicated expression for the intercept of the 'Mk II' straight contour with the y-axis; thereafter the θ-contours for any (P, ϕ)-fixed 2-dimensional slice of C may be computed as before, the bifurcation set again appearing as their envelope. This is illustrated for the Mk I type (Figs. 3 and 4) and the Mk II type (Fig. 5) for $P = Q = 2R$ and several values of ϕ. $J = 2R$ for Fig. 3; Figs. 4 and 5 were drawn with $J = R$ but as mentioned in ((1), p. 222) for a Mk II type machine J is purely a scale factor, so that this difference is unimportant.

In each case it is clear that as ϕ increases from O the first change is that the bottom

https://doi.org/10.1017/S0305004100052348 Published online by Cambridge University Press

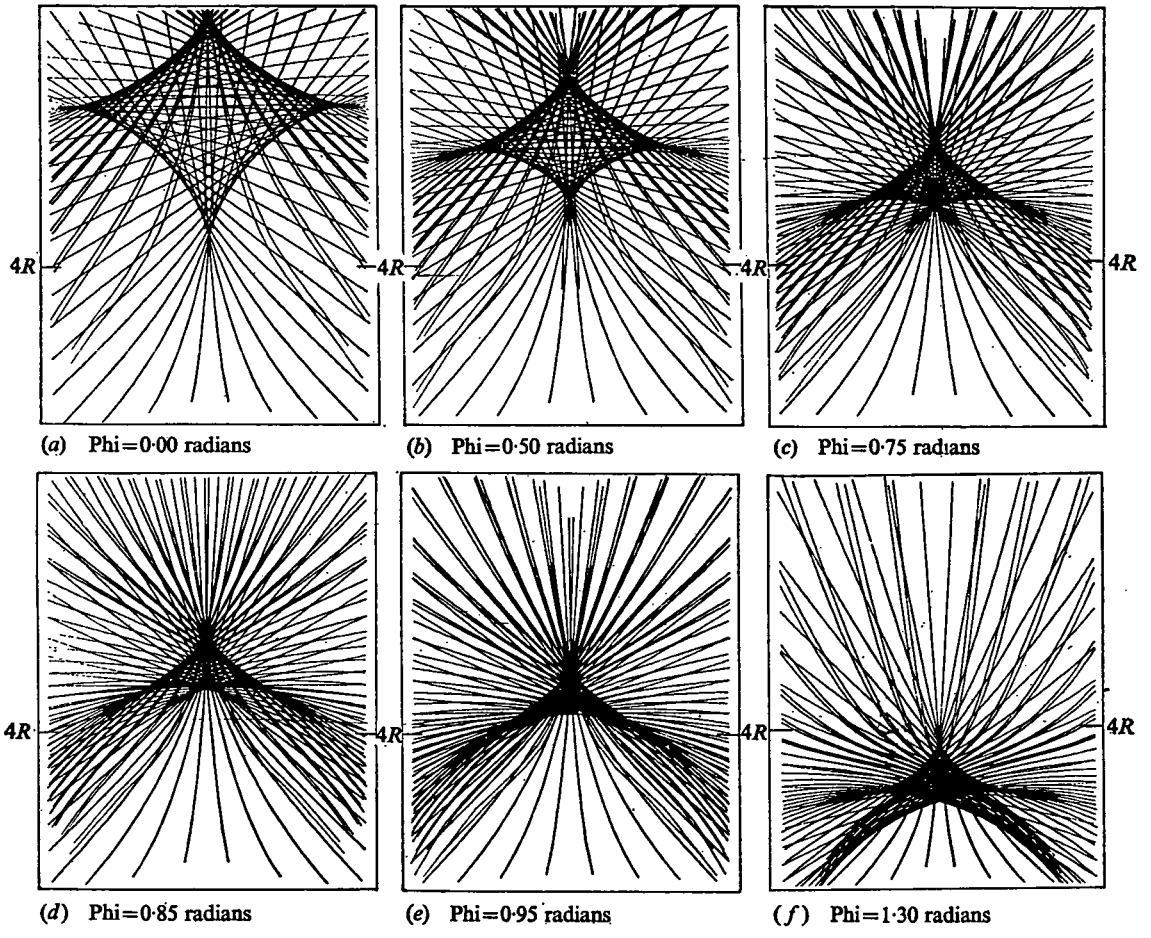

Fig. 3 (*a–f*). Diagram of equilibrium contours for the Mk I machine. $J = P = Q = 2R$; ϕ takes the values (*a*) 0·00 radians, (*b*) 0·50 radians, (*c*) 0·75 radians, (*d*) 0·85 radians, (*e*) 0·95 radians, and (*f*) 1·30 radians, respectively; for further details, see text.

cusp (labelled B in Fig. 6) exfoliates into a complex of three cusps B_1, B_2, B_3 corresponding to the effect of A becoming negative on the $B = 0$, (C, D)-plane diagrams of Fig. 7 (taken from (3), p. 21). This produces a region in which, instead of the two maxima and two minima possessed by the wheel for control points inside the original four-cusped area, it now has three of each. With the control point held in this region, then, the wheel has three stable equilibria. The next development is that this region increases in size, until its boundary PSB_1Q meets the rest of the bifurcation set. Succeeding changes then differ for the two machines: Fig. 3 shows no change in topological type up to $\phi = 1{\cdot}30$, but another butterfly catastrophe is apparent in Fig. 5. A first look at Fig. 5 suggests that the changes simply reverse, but in fact the curves labelled B_1B_2, B_1B_3 in Fig. 6 cross TL, TR, so that the 3-stable equilibria region K now has T as its upper cusp. K then dwindles, to vanish at a second butterfly point where a new cusp B' appears.

https://doi.org/10.1017/S0305004100052348 Published online by Cambridge University Press

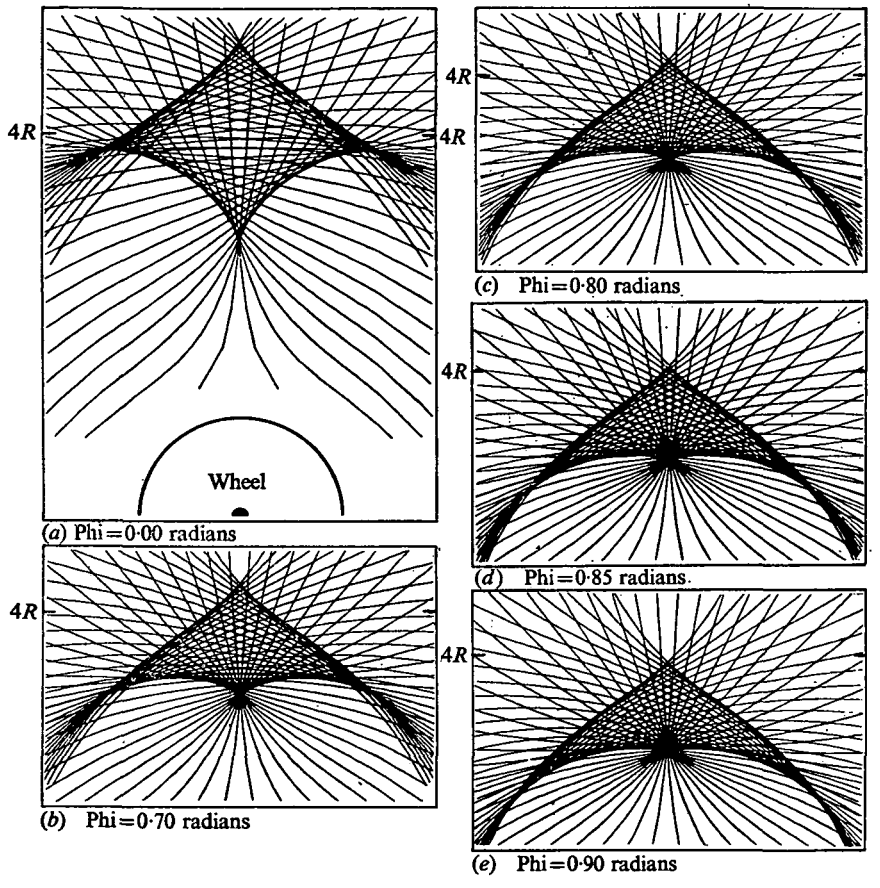

Fig. 4 ($a-e$). Diagram of equilibrium contours for the Mk I machine $J = R, P = Q = 2R$. ϕ takes the values (a) 0·00 radians, (b) 0·70 radians, (c) 0·80 radians, (d) 0·85 radians, (e) 0·90 radians; for further details, see text.

The situation now reached differs more from the $\phi = 0$ one by somewhat more than the 'turning upside down' that a comparison of Figs. 5a, 5l would suggest. Cusps T and B are 'standard' cusps, involving a sheet of minima folding over itself, to produce a layer of maxima between two of minima; L and R are 'dual' cusps, with the role of maxima and minima reversed. The phenomenology of these two situations is very different: suppose in Fig. 7 the control point is moved around the circle C, starting at point I. If the cusp is a standard one, the result will be a jump increase in x as the point passes J, if x started in the lower of its stable equilibria at I, followed by a steady decrease as we move around the circle until it reaches J and jumps again. (This illustrates the way a cusp can model the governing of a jump process by a smooth one; for example if dx/dt is interpreted as electrical potential, a steady cyclic change around C produces an output of regularly spaced 'spike' signals in the manner of a nerve cell.) If the cusp is of the dual type, with the control point at I the only stable equilibrium has x given by the middle layer. As we pass J, we leave the region of control values for

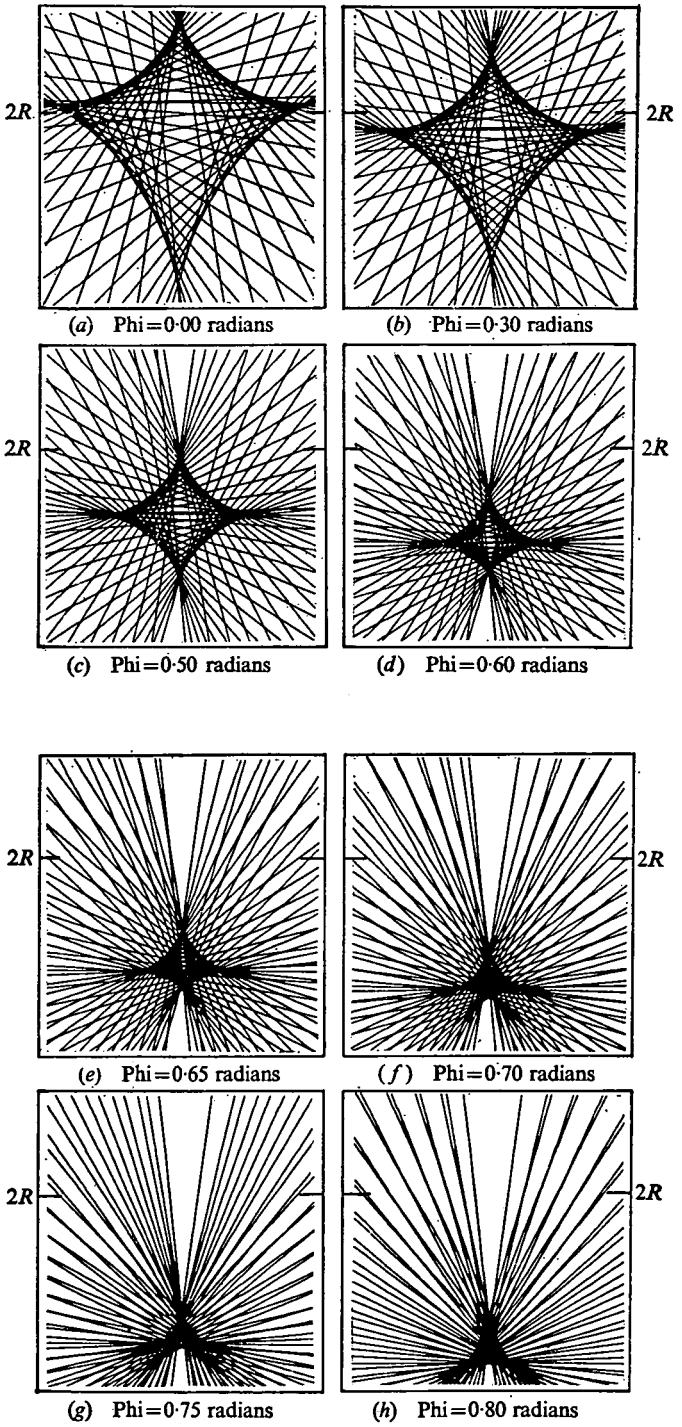

Fig. 5. Continued on next page.

https://doi.org/10.1017/S0305004100052348 Published online by Cambridge University Press

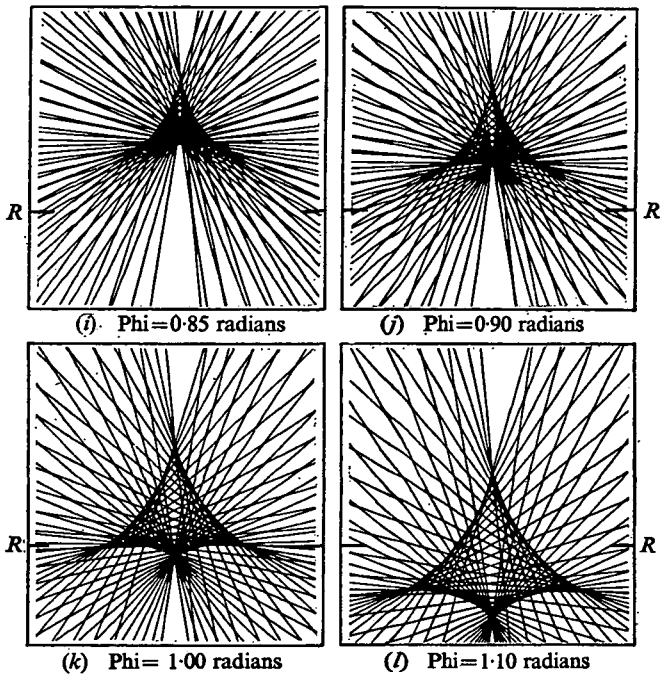

Fig. 5. Diagram of equilibrium contours for the Mk II machine. $J = R$, $P = Q = 2R$. ϕ takes the values (*a*) 0·00 radians, (*b*) 0·30 radians, (*c*) 0·50 radians, (*d*) 0·60 radians, (*e*) 0·65 radians, (*f*) 0·70 radians, (*g*) 0·75 radians, (*h*) 0·80 radians, (*i*) 0·85 radians, (*j*) 0·90 radians, (*k*) 1·00 radians, (*l*) 1·10 radians; for further details, see text.

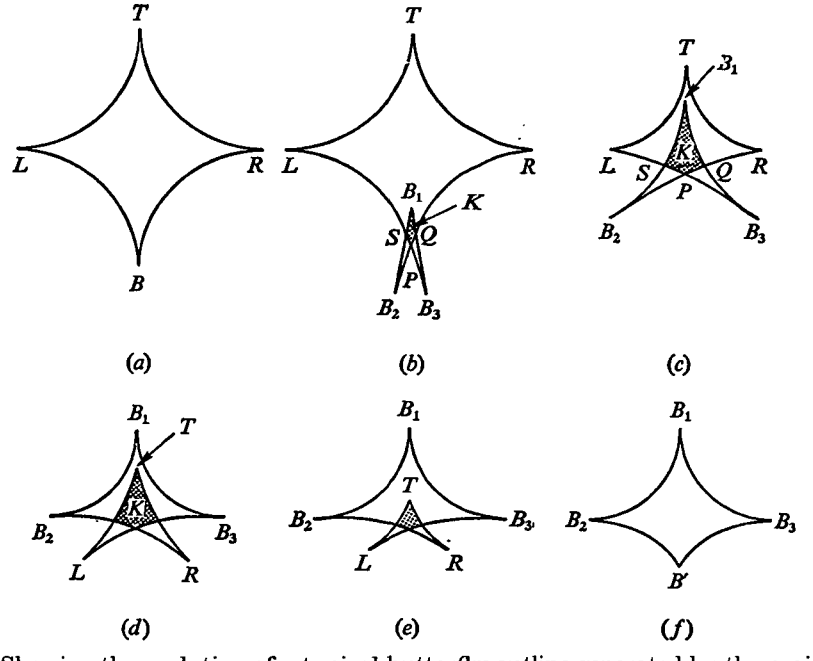

Fig. 6. Showing the evolution of a typical butterfly outline generated by the projection of the surface generated by the equilibrium contours of the Mk II machine (from Fig. 5). For further details, see text.

https://doi.org/10.1017/S0305004100052348 Published online by Cambridge University Press

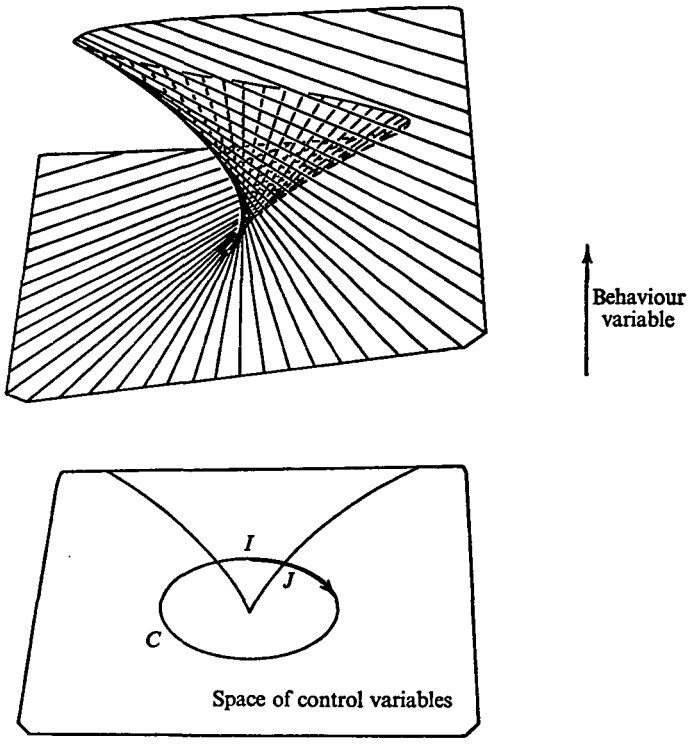

Fig. 7. Showing the three-dimensional nature of the bottom cusp of Fig. 5(*a*) and its projection onto the space of control variables (modified in part from Woodcock and Poston (**2**)).

which stable equilibria exist, and the value of x must jump out of the picture of Fig. 7 entirely. In general it will land in another sheet of the complete surface (cf. Fig. 3 of (**1**)) and never return it to its initial value. If C is a circle around the dual cusp L in Fig. 6*a*, say, entirely left of the y-axis, subsequent behaviour will involve no sudden changes at all. (Physically, the wheel will jump out of its position with the point of attachment of the strings to the right of the y-axis, and thereafter move gently up and down on the left as the control goes around C.)

Now of the new cusps developed from B, as ϕ increases, B_2 and B_3 are standard, while B_1 is dual. These retain their character, and the cusp B' into which T, L, R are transformed at the second butterfly point is dual. Thus the net change from 6*a* to 6*f* is topologically one of interchanging the two types of cusp.

Machines for other catastrophes. Since this catastrophe involves two continua of swallowtails (cf. (**3**)), a suitable reduction of the machine to a three-dimensional control space lying in C and not including the butterfly point itself would serve as a Swallowtail Machine. We thus have concrete physical examples of all four cuspoids among Thom's seven catastrophes (No. 1, the fold, being included in *all* other catastrophes as a section; or it may easily be given a machine to itself). An Elliptic, Hyperbolic, or Parabolic Machine would be interesting to analyse; its behaviour would

have to vary in a space of at least two dimensions, and be controlled through at least three. Moreover, it is unlikely that its singularity structure would involve only one highest-order singularity and the continua of lower-order ones organized by it. The first machine invented to illustrate the cusp catastrophe, the Zeeman device (2), illustrates it in four copies; several subsequent machines have had as many, though simpler examples have been devised. Similarly, this machine involves more than one butterfly catastrophe.

A Parabolic Machine would include examples of all the other catastrophes on Thom's list except the butterfly. (8).

Such machines, particularly if of reasonably simple construction, are of great value in conveying a feel for the interaction of behaviour with this kind of geometry when mathematicians are communicating with scientists from less abstract disciplines.

Added in proof. We learn that 'simultaneous mode design' in Civil Engineering consists precisely of arranging catastrophes with two essential behaviour variables (i.e. umbilic catastrophes), or even more. When an incomplete set of control (in this context *load* and *imperfection*) parameters are used, 'catastrophe' may regain its ordinary meaning. Thompson and Hunt, who have heuristically developed much of Thom theory independently, give (9) elliptic and hyperbolic machines. The hyperbolic is more than just a concrete example like that analysed above; it is a principal component in box girder bridges, and experimentally confirmed analysis predicts that small structural imperfections can greatly reduce the load for which collapse occurs.

Acknowledgement. The authors would like to record their gratitude to Professor E. C. Zeeman, Mathematics Institute, University of Warwick, Coventry, England, for encouraging their study of Castastrophe Theory and his continued interest in and assistance with their work on this subject.

REFERENCES

(1) Poston, T. and Woodcock, A. E. R. Zeeman's Catastrophe Machine. *Proc. Camb. Philos. Soc.*, **74** (1973), 217–226.

(2) Zeeman, E. C. A Catastrophe Machine. In *Towards a Theoretical Biology*, vol. 4 (Ed. by C. H. Waddington, Edinburgh University Press), (1972), 276–282.

(3) Woodcock, A. E. R. and Poston, T. A Geometrical study of the elementary catastrophes. *Springer-Verlag Lecture Notes in Mathematics*, **373** (Berlin, 1974).

(4) Barit, W. Personal communication.

(5) Dubois, Jean-Guy et Dufour, Jean-Paul. La theorie des catastrophes. II. Dynamiques gradients à une variable d'état. *Ann. Inst. H. Poincaré*, **xx** (1974), 135–151.

(6) Zeeman, E. C. The classification of elementary catastrophes of codimension $\leqslant 5$, *University of Warwick Lecture Notes* (written and revised by D. J. A. Trotman).

(7) Dubois Jean-Guy et Dufour, Jean-Paul. La théorie des catastrophes. I. La machine à catastrophes. *Ann. Inst. H. Poincaré*, **xx** (1974), 113–134.

(8) Thom, R. *Stabilité structurelle et morphogenese* (Benjamin, Reading, 1972).

(9) Thompson, J. M. T. and Hunt, G. W. Toward a unified bifurcation theory. *J. App. Math & Phys.* (ZAMP), **26** (1975).